

Spin dynamics of the organic linear chain compounds (TMTTF)₂X (X = SbF₆, AsF₆, BF₄, ReO₄, and SCN)

B. Salameh,^{1,2} S. Yasin,¹ M. Dumm,¹ G. Untereiner,¹ L. Montgomery,³ and M. Dressel¹

¹*Physikalisches Institut, Universität Stuttgart, Pfaffenwaldring 57, D-70550 Stuttgart, Germany*

²*Department of Applied Physics, Tafila Technical University, Tafila, Jordan*

³*Department of Chemistry, Indiana University, Bloomington, Indiana 47405, USA*

(Received 12 September 2010; revised manuscript received 21 March 2011; published 24 May 2011)

We have performed a comprehensive investigation on the spin susceptibility of the organic quantum-spin systems (TMTTF)₂X (X = SbF₆, AsF₆, BF₄, ReO₄, and SCN) in the temperature range from $T = 1.8$ up to 380 K. At elevated temperatures, the spin susceptibility at constant volume $(\chi_s)_V$ can be described by a spin- $\frac{1}{2}$ antiferromagnetic Heisenberg chain with exchange constants J between 400 and 460 K. Below $T \approx 100$ K, slight deviations from the model occur due to interchain interaction. At low temperatures, the compounds undergo transitions to various ordered states of structural or magnetic origin that are discussed in detail. The spin-dimerized ground states of (TMTTF)₂AsF₆ and (TMTTF)₂BF₄ can be described by an alternating spin chain with a singlet-triplet energy gap $\Delta_\sigma(0) = 34.8$ and 52 K, respectively. In (TMTTF)₂ReO₄, however, the spin susceptibility in the anion-ordered state deviates from this model and obeys an activated law with $\Delta_\sigma = 1100$ K. In the antiferromagnetic ground states of (TMTTF)₂SbF₆ and (TMTTF)₂SCN an increase of the spin susceptibility is observed at the lowest temperatures.

DOI: 10.1103/PhysRevB.83.205126

PACS number(s): 75.10.Pq, 75.25.-j, 75.40.Cx, 75.30.Fv

I. INTRODUCTION

Low-dimensional electronic systems such as organic charge-transfer salts are in the focus of ongoing scientific research because many of their properties are not observed in three-dimensional matter but are particular to the reduced dimensionality of those structures. The high anisotropy of these materials influences not only the charge transport, but also leads to several kinds of unusual ground states. The competition between the kinetic energy of electrons, electron-phonon interaction, spin-lattice coupling, magnetic exchange interaction, and electron-electron interaction in the linear chain compounds produces different phases at low temperatures such as charge-density wave (CDW), spin-density wave (SDW), spin-Peierls phase (SP), charge-order state (CO), and superconductivity (SC). Benchmark materials for low-dimensional systems are the quasi-one-dimensional Bechgaard and Fabre salts (TMTSF)₂X and (TMTTF)₂X, where TMTSF and TMTTF denote tetramethyltetraselenafulvalene and tetramethyltetrathiafulvalene, respectively, and X = PF₆, SbF₆, AsF₆, BF₄, ClO₄, ReO₄, Br, or SCN are monovalent anions. The magnetic and electronic properties and the dimensionality of these materials can be easily varied either by exchanging the anions X or by applying external pressure, so the ground states in the phase diagram can be nicely tuned over a large range.¹⁻³ In Fig. 1 the phase diagram is sketched for TMTTF and TMTSF salts with centrosymmetric anions.⁵

The quasi-one-dimensional electronic behavior of (TMTTF)₂X salts originates from their crystallographic structure. The planar TMTTF molecules stack in a zig-zag configuration along the highest conducting direction (*a* axis). They form layers in the *ab* plane which alternate with the anion X along the *c* direction. Moreover, the stacks are not regular, in the sense that the TMTTF molecules form dimers along the *a* axis.⁶ The dimerization of the TMTTF

molecules along the chain has drastic consequences on the electronic properties of these salts because it enhances the charge localization. Due to their smaller transfer integrals t and large onsite Coulomb repulsion U ,⁷⁻¹⁰ TMTTF salts are Mott insulators. The broad minimum in resistivity observed in the temperature range $100 \text{ K} \leq T \leq 300 \text{ K}$ is attributed to a continuous $4k_F$ charge localization due to the anion potential.^{11,12}

The anions X are incorporated in cavities delimited by the TMTTF molecules. They are either centrosymmetric (spherical or octahedral), such as PF₆, AsF₆, SbF₆, or Br, tetrahedral such as ClO₄, ReO₄, or BF₄, or linear (SCN). The noncentrosymmetric anions have two (or more) equivalent orientations corresponding to short and long contacts between the sulfur atoms of the TMTTF molecule and the peripheral electronegative atom of the anion. Although at room temperature these noncentrosymmetric anions are randomly orientated, in general, an orientational ordering occurs upon cooling,⁶ leading to a superstructure with the critical wave vector $\mathbf{Q}_{AO} = (1/2, 1/2, 1/2)$. X-ray studies have shown that (TMTTF)₂BF₄ and (TMTTF)₂ReO₄ undergo a first-order structural phase transition due to anion ordering at $T_{AO} = 41.5$ and 157 K, respectively.^{6,12,13} The transition is accompanied by a shift of the anions from the center of the cavity delimited by the organic molecules that causes a sizable tetramerization of the organic stacks. This is not the case in (TMTTF)₂SCN, which has an anion-ordering transition at 160 K with a $(0, 1/2, 1/2)$ critical wave vector.¹⁴ This means the structure is not perturbed along the stacking direction and there is no tetramerization of the organic stacks. Centrosymmetric anions, such as AsF₆, SbF₆, and Br, cannot exhibit anion ordering. The (TMTTF)₂AsF₆ salt undergoes a spin-Peierls transition at $T_{SP} = 13$ K (Ref. 16) while (TMTTF)₂SbF₆ and (TMTTF)₂SCN have an antiferromagnetic (AFM) ground state at $T_N = 8$ and 7 K, respectively.^{11,14} Measuring a series of alloys (TMTTF)₂[(AsF₆)_x(SbF₆)_{1-x}], Iwase *et al.*

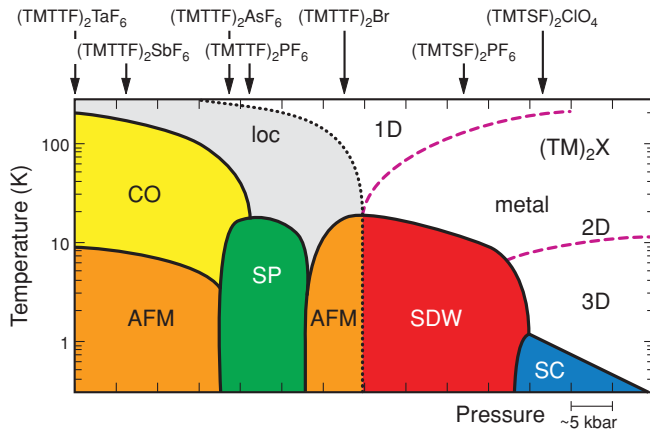


FIG. 1. (Color online) The phase diagram of the quasi one-dimensional TMTTF and TMTSF salts, first suggested by Jérôme and coworkers⁴ and further supplemented by many groups over the years.³ For the different compounds with centrosymmetric anions the ambient-pressure position in the phase diagram is indicated.⁵ Going from the left to the right, the materials get less one-dimensional due to the increasing interaction in the second and third direction. At low temperatures various broken-symmetry ground states develop. Here loc stands for charge localization, CO for charge ordering, SP for spin-Peierls, AFM for antiferromagnet, SDW for spin density wave, and SC for superconductor. While some of the boundaries are clear phase transitions, the ones indicated by dashed lines are better characterized as a crossover. The position in the phase diagram can be tuned by external or chemical pressure.

investigated the magnetic properties at the boundary between the antiferromagnetic and spin-Peierls phases and proposed a quantum critical behavior.¹⁵ While the magnetic properties of $(\text{TMTCF})_2X$ ($C = \text{S, Se}$ and $X = \text{PF}_6, \text{AsF}_6, \text{ClO}_4$, and Br) have been characterized in Refs. 17 and 18, in the present paper we report on detailed magnetic investigations on five salts from the TMTTF family with $X = \text{SbF}_6, \text{AsF}_6, \text{BF}_4, \text{ReO}_4$, and SCN in the normal paramagnetic state and in the ordered ground states.

II. EXPERIMENTAL DETAILS

Single crystals of $(\text{TMTTF})_2X$ ($X = \text{SbF}_6, \text{AsF}_6, \text{BF}_4, \text{ReO}_4$, and SCN) were grown by the standard electrochemical growth procedure outlined previously.¹⁹ The magnetic susceptibility measurements of $(\text{TMTTF})_2\text{SbF}_6$, $(\text{TMTTF})_2\text{AsF}_6$, $(\text{TMTTF})_2\text{BF}_4$, and $(\text{TMTTF})_2\text{SCN}$ were performed using a Quantum Design superconducting quantum interference device (SQUID) magnetometer between 1.8 and 380 K. A large amount of crystals of each compound is needed to perform the susceptibility measurement. The single crystals were glued parallel to each other inside a plastic straw using vacuum grease and the magnetic field was applied parallel to the a axis. The background signal of the sample holder and the vacuum grease was measured separately and subtracted in order to obtain the intrinsic magnetization of the sample. To estimate the spin susceptibility, we further subtracted the diamagnetic contribution of the core electrons $\chi_{\text{dia}} = -5.3 \times 10^{-9} \text{ m}^3/\text{mole}$ from the original data. Since the temperature-independent diamagnetic contribution mainly stems from the

TMTTF molecules, the value of the core susceptibility was assumed to be independent of the monovalent anion and we used the same value of the χ_{dia} to calculate the spin susceptibility of all the salts investigated. For $(\text{TMTTF})_2\text{ReO}_4$, we carried out an electron spin resonance (ESR) measurement utilizing a continuous-wave X -band spectrometer (Bruker ESR 300) at 9.5 GHz equipped with an Oxford ESR 900 cryostat for temperature measurements between 4.2 and 300 K. The sample was glued to a quartz rod by paraffin along its a axis. We use the TE_{102} mode of a rectangular cavity. The spin susceptibility was determined by comparing the intensity of the measured ESR signal with that of DPPH (2,2-diphenyl-1-picrylhydrazyl).

III. RESULTS

The temperature dependence of the spin susceptibility at constant pressure $\chi_s(T)$ of the investigated compounds is plotted in Fig. 2. For all salts investigated, the room temperature value is nearly independent of the counter ions and falls in the range of 5×10^{-4} to $6 \times 10^{-4} \text{ emu/mole}$, in good agreement with previous data.^{11,17}

The spin susceptibility of $(\text{TMTTF})_2\text{SbF}_6$ [Fig. 2(a)] increases by cooling down from 380 K. At $T = 315 \text{ K}$, $\chi_s(T)$ exhibits a smooth maximum and then begins to decrease continuously by further lowering the temperature without any obvious change at the charge-localization temperature $T_\rho = 240 \text{ K}$ or at the charge-order temperature $T_{\text{CO}} = 157 \text{ K}$. Eventually the spin susceptibility exhibits a strong drop by decreasing the temperature from 16 K down to $T_N = 8 \text{ K}$ below which the susceptibility begins to increase with decreasing the temperature [see the insert of Fig. 2(a)].

At high temperatures, $\chi_s(T)$ for the other four salts is very similar to the result of $(\text{TMTTF})_2\text{SbF}_6$. In all cases the susceptibility decreases continuously below room temperature, without any obvious change at the charge-localization temperature T_ρ .^{11,16,20} $(\text{TMTTF})_2\text{AsF}_6$ undergoes a spin-Peierls transition at $T_{\text{SP}} = 13 \text{ K}$ below which the spin susceptibility decreases rapidly upon reducing the temperature, as expected for a

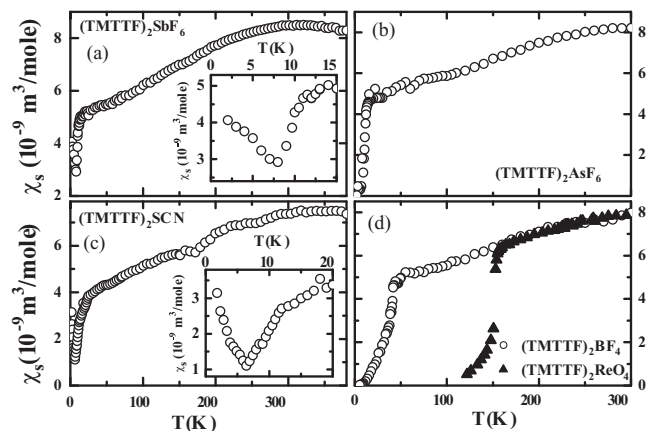


FIG. 2. Temperature dependence of the spin susceptibility at constant pressure of $(\text{TMTTF})_2X$, $X = \text{SbF}_6, \text{AsF}_6, \text{SCN}, \text{BF}_4$, and ReO_4 , along the a axis. The insets of panels *a* and *c* give enlarged views of the spin susceptibility near the Néel temperature of $(\text{TMTTF})_2\text{SbF}_6$ ($T_N = 8 \text{ K}$) and $(\text{TMTTF})_2\text{SCN}$ ($T_N = 7 \text{ K}$).

second-order phase transition to a nonmagnetic ground state. The susceptibility does not vanish completely down to 1.8 K. No obvious effect of the charge-ordering transition at $T_{CO} = 102$ K is detected in $\chi_s(T)$. Above the antiferromagnetic phase transition, we observe the same behavior of the spin susceptibility in $(\text{TMTTF})_2\text{SCN}$ as in $(\text{TMTTF})_2\text{SbF}_6$: $\chi_s(T)$ begins to decrease rapidly upon cooling below about 20 K and it increases again for reducing the temperature below $T_N = 7$ K [see the insert of Fig. 2(c)]. At the anion-ordering temperature $T_{AO} = 160$ K of $(\text{TMTTF})_2\text{SCN}$ a small dip in the susceptibility is observed, although no tetramerization of the TMTTF anions is expected along the stacks since the component of the anion-ordering wave vector along the stacking direction is zero [$\mathbf{Q}_{AO} = (0, 1/2, 1/2)$].¹⁴ This dip might be caused by rearranging the spins in the perpendicular plane due to the anion-ordering transition. The anion ordering in $(\text{TMTTF})_2\text{BF}_4$ and $(\text{TMTTF})_2\text{ReO}_4$ [$\mathbf{Q}_{AO} = (1/2, 1/2, 1/2)$] leads to a first-order structural phase transition at $T_{AO} = 41$ and 156 K, respectively.^{6,13} This transition is accompanied by tetramerization of the TMTTF chain along the stacking direction and leads to a step-like decrease of the spin susceptibility at T_{AO} followed by an exponential decrease of $\chi_s(T)$, as expected for a phase transition to a nonmagnetic ground state. The susceptibility does not vanish down to 1.8 K for $(\text{TMTTF})_2\text{BF}_4$ while it vanishes completely in $(\text{TMTTF})_2\text{ReO}_4$ at 122 K.

IV. ANALYSIS AND DISCUSSION

A. High-temperature paramagnetic region

Before analyzing the results, let us recall the spin structure of the Fabre salts in the high-temperature paramagnetic region. In $(\text{TMTTF})_2X$, the transfer of one electron from two donor molecules to each anion leaves on average half a hole per TMTTF molecule. Therefore, these salts are expected to be metals with a 3/4 filled conduction band. However, dimerization of the TMTTF molecules along the chain direction produces a half-filled band with one hole per TMTTF dimer. Due to the large onsite Coulomb repulsion the charge carriers are localized; a Mott-Hubbard gap in the electronic excitation spectrum drives these compounds insulating. The spins are sitting on the dimers and are localized in the chain direction. They arrange themselves in an antiparallel fashion with respect to each other, forming a uniform antiferromagnetic (AFM) Heisenberg chain.

Organic radical salts have relatively large thermal expansion coefficients. For example, by heating a single crystal of $(\text{TMTSF})_2\text{PF}_6$ from 4 up to 300 K, the a axis elongates by $\Delta a/a = 0.03$, along the b axis $\Delta b/b = 0.01$, and along the c axis $\Delta c/c = 0.01$.^{21,22} The expansion coefficient of the a axis for $(\text{TMTSF})_2\text{PF}_6$ increases linearly with temperature above 100 K with a slope of $(\Delta a/a)/T = 10^{-4}$ with distinct anomalies due to the various transitions.^{22,23} The large thermal expansion along the chain direction significantly effects the temperature dependence of the spin susceptibility. To compare the experimental results [which are obtained at constant pressure $(\chi_s)_p$] with the theoretical calculations [which are obtained at constant volume $(\chi_s)_v$], the spin susceptibility at constant pressure has to be transformed to the spin suscep-

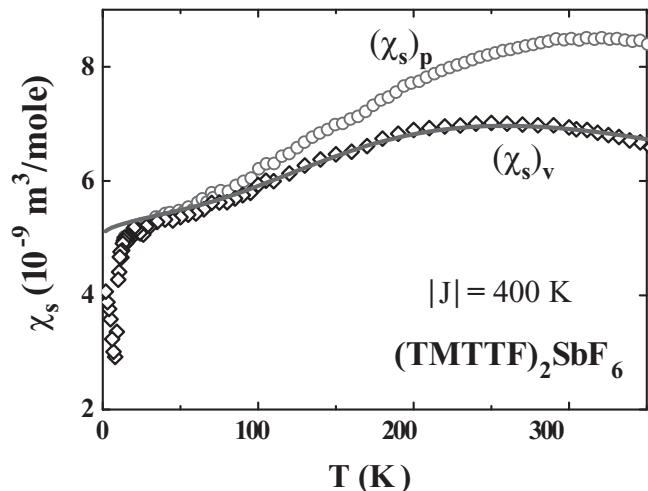


FIG. 3. (Color online) Temperature dependence of the spin susceptibility at constant pressure $(\chi_s)_p$ (red circles) and at constant volume $(\chi_s)_v$ (diamonds) of $(\text{TMTTF})_2\text{SbF}_6$ calculated from SQUID measurements along the stacking direction a . The line corresponds to a fit using the model by Eggert, Affleck, and Takahashi²⁷ for an $S = 1/2$ AFM Heisenberg chain with $J = 400$ K.

tibility at constant volume. In the case of $(\text{TMTSF})_2\text{PF}_6$ the temperature dependence of $(\chi_s)_v$ was estimated by Wzietek *et al.* by performing nuclear magnetic resonance (NMR) and x-ray measurements under pressure.²⁴ Here we assume that the substitution of selenium by sulfur as well as exchanging the inorganic anion has no influence on the expansion coefficient of the material; the same procedure has been applied in previous investigations of other $(\text{TMTTF})_2X$ and $(\text{TMTSF})_2X$ salts.^{17,25,26} Therefore, we took the same ratio $(\chi_s)_v/(\chi_s)_p$ to rescale the susceptibility data for the investigated TMTTF salts.

The temperature dependence of $(\chi_s)_v$ and $(\chi_s)_p$ of $(\text{TMTTF})_2\text{SbF}_6$, for instance, is presented in Fig. 3. The smooth maximum of $(\chi_s)_p(T)$ at about $T = 315$ K shifts down to 255 K for $(\chi_s)_v(T)$. The spin susceptibility at constant volume of $(\text{TMTTF})_2\text{SbF}_6$ resembles the well-known behavior of a spin- $1/2$ Heisenberg chain with AFM exchange coupling. The spin susceptibility of such a system was investigated theoretically by Bonner and Fisher²⁸ and by Eggert, Affleck, and Takahashi (EAT model).²⁷ For example, the high-temperature $(\chi_s)_v(T)$ of $(\text{TMTTF})_2\text{SbF}_6$ for $T \geq 100$ K can be modelled numerically using²⁹

$$\chi(T) = \frac{A}{T} \frac{0.25 + Bx + Cx^2}{1 + Dx + Ex^2 + Fx^3}, \quad (1)$$

with numerical constants B, C, D, E, and F, $A = Ng^2\mu_B^2/k_B$, $x = J/T$, and $J = 400$ K. The excellent agreement of the high-temperature susceptibility data with an $S = 1/2$ AFM Heisenberg chain with localized spins confirms previous measurements on $(\text{TMTTF})_2\text{PF}_6$ and $(\text{TMTTF})_2\text{Br}$.¹⁷ The crossover from weak metallic to insulating behavior observed in transport measurements^{12,30} around 100 to 300 K, while the spin degrees of freedom remain gapless in these compounds, can be considered as strong evidence that the spin and charge degrees of freedom are decoupled.^{31,32} Indications for the

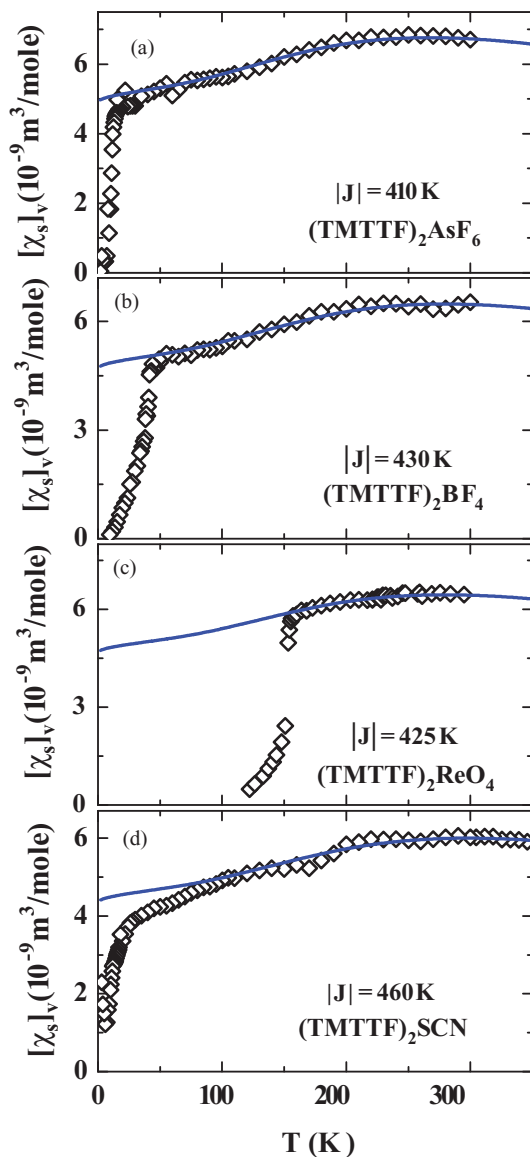


FIG. 4. (Color online) Temperature dependence of the spin susceptibility at constant volume $(\chi_s)_V$ of (a) $(\text{TMTTF})_2\text{AsF}_6$, (b) $(\text{TMTTF})_2\text{BF}_4$, (c) $(\text{TMTTF})_2\text{ReO}_4$, and (d) $(\text{TMTTF})_2\text{SCN}$ calculated from SQUID and ESR measurements along the stacking direction a . The lines correspond to fits using the EAT model for the $S = 1/2$ AFM Heisenberg chain²⁷ with $J = 410, 430, 425,$ and 460 K for the $X = \text{AsF}_6, \text{BF}_4, \text{ReO}_4,$ and SCN salts, respectively.

separation of spin and charge were also seen by photoemission spectroscopy in other one-dimensional organic conductors, such as TTF-TCNQ.^{33,34} Therefore, the Bonner-Fisher model of localized spins is applicable.

In Fig. 4 the temperature dependence of the spin susceptibility at constant volume $(\chi_s)_V$ is shown for the other $(\text{TMTTF})_2X$ salts investigated. In all cases $(\chi_s)_V(T)$ decreases gradually by lowering the temperature after passing a maximum value at 263 K ($X = \text{AsF}_6$), 275 K (BF_4), 273 K (ReO_4), and 295 K (SCN). At high temperatures ($T \geq 100$ K)³⁵ the behavior $(\chi_s)_V(T)$ of the four salts can also be described by the models of Eggert, Affleck, and Takahashi²⁷ or Bonner and Fisher²⁸ with $J = 410, 430, 425,$ and 460 K

for $(\text{TMTTF})_2\text{AsF}_6$, $(\text{TMTTF})_2\text{BF}_4$, $(\text{TMTTF})_2\text{ReO}_4$, and $(\text{TMTTF})_2\text{SCN}$, respectively. The uncertainty of determining the exchange coupling J by this fit is about ± 3 K for all cases. The effective exchange interaction was estimated qualitatively by Hotta.³⁶ Since T_{CO} is higher for $(\text{TMTTF})_2\text{ReO}_4$ compared to $(\text{TMTTF})_2\text{BF}_4$ and the charge disproportionation is larger, she suggested that nearest-neighbor interaction V is stronger in the ReO_4 compound compared to the BF_4 analog. The large V reduces the effective magnetic interaction and thus explains the slightly smaller value of $J = 425$ K observed in $(\text{TMTTF})_2\text{ReO}_4$, while for $(\text{TMTTF})_2\text{BF}_4$ we find $J = 430$ K.

For all compounds investigated, $(\chi_s)_V(T)$ begins to deviate from the EAT model below approximately 100 K, where the measured susceptibility becomes smaller than the theoretical value. This deviation can be due to the two-dimensional character of the $(\text{TMTTF})_2X$ salts below about 100 K where the interchain transfer integral in these salts is about $t_b \approx 12$ meV, corresponding to 130 K. Fuseya *et al.* theoretically investigated the role of interchain hopping on the magnetic properties and found that t_\perp enhances the antiferromagnetic spin fluctuations at low temperatures, while it suppresses the one-dimensional fluctuations at high temperatures.³⁷ When looking at the b - and c -axis unit cell parameters, we find a steady decrease when going from $X = \text{SbF}_6$, via AsF_6 and ReO_4 , to BF_4 , implying an increase in t_\perp . To learn more about the role of interchain hopping on the magnetic susceptibility, it is highly desirable to conduct pressure-dependent measurements of $\chi_s(T)$.

The obtained values of the AFM exchange constant J for different $(\text{TMTTF})_2X$ listed in Table I together with data from Refs. 17, 25, and 26 are plotted in Fig. 5 as a function of the unit cell dimension a along the stacking direction (i.e., the distance between two adjacent spins). With increasing unit cell length a , the coupling J decreases in an almost linear way. This is expected because, with increasing distance between the TMTTF molecules, the overlap between the orbital wave functions decreases. However, to our knowledge there exists no theoretical model to describe this behavior.

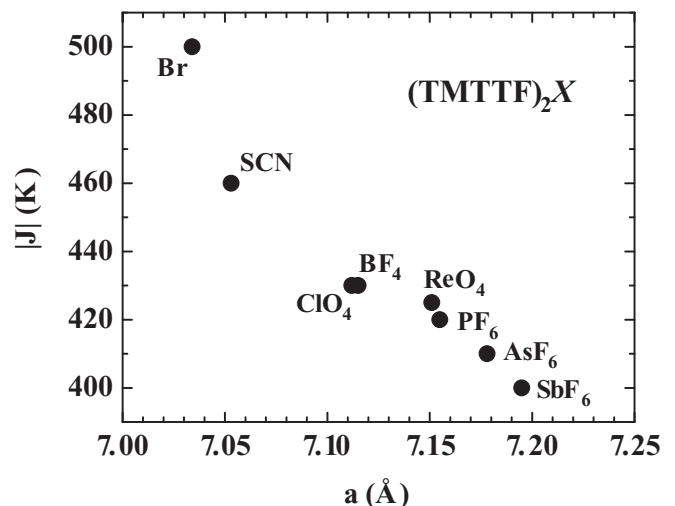


FIG. 5. Relation between the exchange constant J and the unit cell dimension along the stacking direction a for different $(\text{TMTTF})_2X$ salts with X as indicated in the figure. We combine the present results with previous investigations.^{17,25,26}

TABLE I. Charge-localization temperatures T_ρ , charge- and anion-ordering temperatures T_{CO} and T_{AO} , respectively, spin-Peierls transition T_{SP} , Néel temperature T_N , and exchange constants J of various Fabre salts $(TMTTF)_2X$ ($X = SbF_6, AsF_6, BF_4, ReO_4,$ and SCN).

Compound	T_ρ (K)	T_{CO} (K)	T_{AO} (K)	T_{SP} (K)	T_N (K)	J (K)
$(TMTTF)_2SbF_6$	240	157			8	400
$(TMTTF)_2AsF_6$	250	102		13		410
$(TMTTF)_2BF_4$	240	84	41			430
$(TMTTF)_2ReO_4$	290	230	157			425
$(TMTTF)_2SCN$	250		160		7	460

B. Charge-localization and charge-order transition

In all compounds investigated, no sign of the resistivity minimum was found in the susceptibility; in other words there is no change of the susceptibility at the localization temperature T_ρ . We pointed out above that this can be seen as evidence of the spin and charge degrees of freedom being decoupled.²

Although the effect of charge ordering on the spin degree of freedom has attracted considerable attention from the theoretical side, it is not completely clear how the spin degrees of freedom behave in the charge-order state and in the metallic state under the influence of charge fluctuations when strong correlations are present. Tanaka and Ogata predict³⁸ that, for $T = 0$, the effective coupling J is suppressed by the effect of the nearest-neighbor Coulomb repulsion V through charge fluctuation and χ_s increases with increasing V ; when the charge-order transition occurs at $V = 2t$ the anomaly is hardly detectable.

In Ref. 12 the influence of charge order on the transport properties of the different $(TMTTF)_2X$ was investigated in all three directions. A correlation was established between the charge-order transition temperature T_{CO} and structural properties, in particular the shortest distance between the ligands of the anions and the sulfur atoms in TMTTF. Thermal expansion measurements provide evidence for the structural changes as well.²² The important point is that we do not find any indication of the charge-order transition in the spin susceptibility $\chi_s(T)$, in accord with our previous investigations.¹⁷ This basically infers that the spins on the chains do not get modified considerably by the charge disproportionation within one dimer. However, we find a significant increase of the ESR linewidth ΔH below T_{CO} and a change in the angular dependence.³⁹ Recently, Furukawa *et al.*⁴⁰ also pointed out the importance of the interaction between the organic cations and the counterions. Their ESR data reveal an anomalous temperature behavior of the g factor, indicating the deformation of the molecular orbitals by the anions potential. Although the distance between neighboring spins along the chain does not change due to the charge order, the three-dimensional nature of the charge rearrangement shows up in a change of the crystal field and causes additional broadening.

C. Spin-Peierls transition in $(TMTTF)_2AsF_6$

The spin-Peierls transition is a second-order phase transition due to a $2k_F$ instability which occurs at a critical temperature $T = T_{SP}$ in a regular $S = 1/2$ Heisenberg antiferromagnetic spin chain. The SP transition is accompanied by lattice modulation, which results in a tetramerization of the molecular chain; this leads to formation of spin-singlet pairs. The spin susceptibility decreases exponentially by lowering the temperature down to $T = 0$ since a singlet-triplet gap opens in the spin excitation spectrum. The temperature dependence of the spin susceptibility of $(TMTTF)_2AsF_6$ in the low-temperature region is shown in Fig. 6. Below $T_{SP} = 13$ K the temperature dependence of the spin susceptibility can be described by Bulaevskii's model for an alternating spin chain:⁴¹

$$\chi_s(T) = \frac{\alpha}{T} \exp\left\{-\frac{J_1\beta}{T}\right\}. \quad (2)$$

The values of α and β are tabulated in Ref. 41 for given alternation parameters γ . In the spin-Peierls state, the spin susceptibility can be fit by Eq. (3) after substituting $J_1\beta$ with $J[1 + \delta(\gamma)]\beta(\gamma) = J\beta'(\gamma)$. Using the obtained value of $J = 410$ K from the Bonner-Fisher model, the alternation parameter γ can be calculated by

$$\gamma(T) = \frac{1 - \delta(T)}{1 + \delta(T)} = \frac{J_2(T)}{J_1(T)}, \quad (3)$$

with $J_1 = J[1 \pm \delta]$. The fit shown as the solid line in Fig. 6 yields $\gamma = 0.94$. The corresponding intradimer and interdimer exchange constants are $J_1 = 423$ K and $J_2 = 397$ K, respectively.

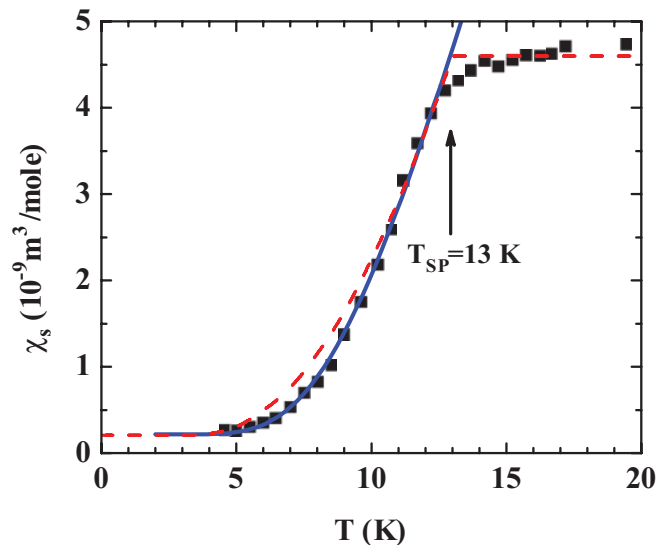


FIG. 6. (Color online) Temperature dependence of the spin susceptibility along the a axis of $(TMTTF)_2AsF_6$ in the low-temperature region. Below $T_{SP} = 13$ K the spin susceptibility drops exponentially, indicating a transition to a nonmagnetic ground state. The blue solid line corresponds to a fit by Bulaevskii's model⁴¹ of the alternating spin chain using Eq. (2) with $\gamma = 0.94$ and $\Delta_\sigma(0) = 34.8$ K. The red dashed line corresponds to the calculations by Orignac and Chitra⁴² with $\Delta_\sigma(0) = 37.5$ K. A constant offset of $0.2 \times 10^{-9} \text{ m}^3/\text{mole}$ accounts for the finite zero-temperature value.

Using the thermodynamic Bethe ansatz to evaluate the finite-temperature free energy of the sine-Gordon Hamiltonian, Orignac and Chitra⁴² calculate the magnetic susceptibility for $T < T_{SP}$:

$$\chi_s(T) = \frac{2}{\pi^2 J} \sqrt{\frac{8\pi \Delta_\sigma(0)}{T}} \exp\left\{-\frac{\Delta_\sigma(0)}{T}\right\}, \quad (4)$$

plus higher-order terms of $T^{-1/2} \exp\{-\Delta_\sigma(0)/T\}$. The fit displayed in Fig. 6 as a dashed line yields $\Delta_\sigma(0) = 37.5$ K, but it is not superior to Bulaevskii's model.

The tetramerization of the spin chain below T_{SP} produces an energy gap Δ_σ between the nonmagnetic singlet ground state and the triplet excited state. The singlet-triplet energy gap is related to the alternation $\delta(T)$ via

$$\Delta_\sigma(T) = 0.8615J[\delta(T)]^{2/3}, \quad (5)$$

where the energy gap Δ_σ is assumed to be temperature dependent:⁴²

$$\Delta_\sigma(T) = \Delta_\sigma(0) \left[1 - \sqrt{\frac{216T}{\pi \Delta_\sigma(0)}} \exp\left\{-\frac{\Delta_\sigma(0)}{T}\right\} \right]. \quad (6)$$

From Eq. (5) the singlet-triplet energy gap in the $T = 0$ limit can be calculated to be $\Delta_\sigma(0) = 34.8$ K. The obtained ratio of the singlet-triplet energy gap to the transition temperature, $\Delta_\sigma(0)/T_{SP} = 2.67$, is in very good agreement with the predictions by second-order perturbation theory of $\Delta_\sigma(0)/T_{SP} = 2.47$.⁴² Using the relation $\Delta_\sigma(0) = 1.637\delta J$,⁴³ we previously⁴⁴ estimated the singlet-triplet energy gap for $(\text{TMTTF})_2\text{AsF}_6$ to be $\Delta_\sigma(0) = 22$ K. A similar analysis as presented here can be applied to the sister compound $(\text{TMTTF})_2\text{PF}_6$ that has a spin-Peierls transition at $T_{SP} = 19$ K and coupling $J = 420$ K with $\delta = 0.0471$.¹⁷ Using Eq. (5) the singlet-triplet energy gap is $\Delta_\sigma(0) = 47.1$ K and thus $\Delta_\sigma(0)/T_{SP} = 2.48$, which is again very close to the theoretical prediction. Here, it is interesting to note that a universal relation of the gap energy to the transition temperature was found that is different from the mean-field-theory prediction of 1.76 because strong interactions cause a renormalization.⁴²

D. Anion ordering in $(\text{TMTTF})_2\text{BF}_4$ and $(\text{TMTTF})_2\text{ReO}_4$

$(\text{TMTTF})_2\text{BF}_4$ and $(\text{TMTTF})_2\text{ReO}_4$ undergo a first-order anion-ordering phase transition at $T_{AO} = 41.5$ and 157 K, respectively. This structural transition is accompanied by a pronounced anomaly in the electrical resistivity,¹² a decrease in the dielectric permittivity,²⁰ and a step-like decrease in the ESR linewidth along the three crystal axes.³⁹ Since the anion-ordering wave vector of $(\text{TMTTF})_2\text{BF}_4$ and $(\text{TMTTF})_2\text{ReO}_4$ is $\mathbf{Q}_{AO} = (1/2, 1/2, 1/2)$, the stacks are tetramerized (i.e., a considerable deformation of the organic stacks takes place).

Figures 7 and 8 show the low-temperature spin susceptibility at constant volume of $(\text{TMTTF})_2\text{BF}_4$ and $(\text{TMTTF})_2\text{ReO}_4$. The most pronounced change in $(\chi_s)_V(T)$ happens at the anion-ordering transition. The step-like behavior at T_{AO} indicates the first-order character of this phase transition. At lower temperatures the spin susceptibility decreases exponentially with temperature. Due to the tetramerization along the donor stacks, two TMTTF dimers carrying spin $\frac{1}{2}$ each become coupled; the system enters a nonmagnetic ground state. For $T < T_{AO}$ the

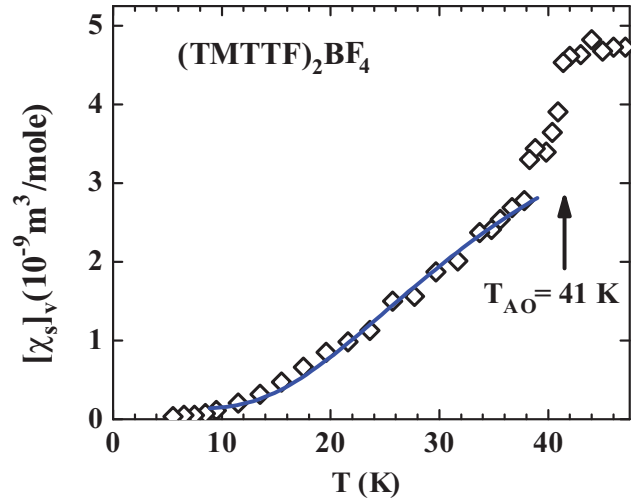


FIG. 7. (Color online) Low-temperature behavior of the spin susceptibility of $(\text{TMTTF})_2\text{BF}_4$ along the a axis. At $T_{AO} = 41$ K a step-like drop in the spin susceptibility is observed, below which the spin susceptibility decreases exponentially, indicating a transition to a nonmagnetic ground state. The line corresponds to a fit by Bulaevskii's model (Ref. 41) of the alternating spin chain using Eq. (2) with $\gamma = 0.90$ and $\Delta_\sigma(0) = 52.0$ K.

spin susceptibility at constant volume of $(\text{TMTTF})_2\text{BF}_4$ can be described by Bulaevskii's model of the alternating spin chain [Eq. (2)] as shown by the solid line in Fig. 7. Using the value

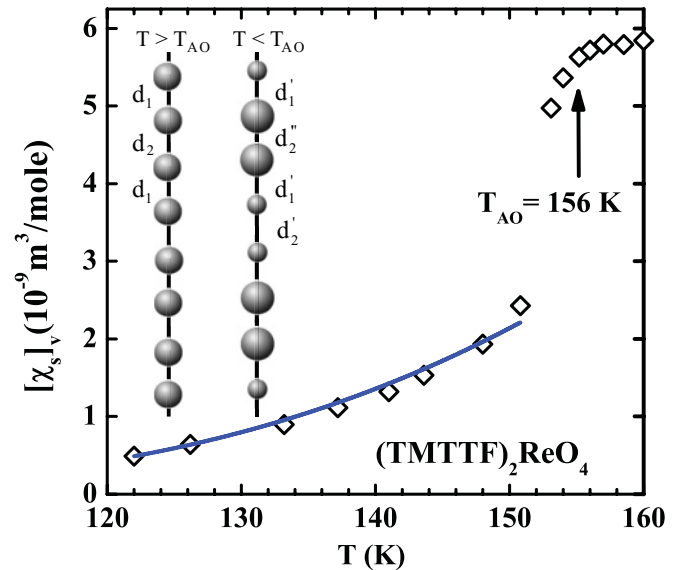


FIG. 8. (Color online) Temperature-dependent spin susceptibility $[\chi_s]_V(T)$ of $(\text{TMTTF})_2\text{ReO}_4$ along the a axis calculated from the ESR measurements. At $T_{AO} = 157$ K a step-like drop in the spin susceptibility is observed below which $[\chi_s]_V(T)$ decreases exponentially, indicating a transition to a nonmagnetic ground state. The solid line corresponds to a fit by an activation law (see text) with $\alpha = 4.9 \times 10^5$ $\text{m}^3\text{K}/\text{mole}$ and $\Delta_\sigma = 1100$ K. The insert depicts a one-dimensional spin chain above and below T_{AO} . d_1 and d_2 are the intradimer and interdimer distances, respectively. The anion-ordering transition leads to considerable deformation of the organic stacks with $d'_1 \approx 3.45$ Å, $d'_2 \approx 3.60$ Å, and $d''_2 \approx 3.48$ Å.⁴⁵ The large circles below T_{AO} indicate larger charge density compared to the small ones.

of the AFM exchange constant $J = 430$ K, which is obtained by fitting the spin susceptibility in the high-temperature region obtained by the Bonner and Fisher model, we get an alternation parameter $\gamma = 0.90$, $J_1 = 452.64$ K, and $J_2 = 407.4$ K via Eq. (3). The singlet-triplet energy gap $\Delta_\sigma = 52.0$ K is given by Eq. (5). In case of $(\text{TMTTF})_2\text{ReO}_4$, the spin susceptibility deviates from Bulaevskii's model due to the high transition temperature and the large dimerization⁶ in this compound. As shown in Fig. 8, below T_{AO} $(\chi_s)_V(T)$ can be fit using an activation law:¹¹

$$\chi_s(T) = \frac{\alpha}{T} \exp\left\{-\frac{\Delta_\sigma}{T}\right\}, \quad (7)$$

where α is the fit parameter. Using $\alpha = 4.9 \times 10^5$ m³K/mole, the singlet-triplet spin gap is calculated to be $\Delta_\sigma = 1100$ K, which agrees well with the value obtained from the magnetization and the x-ray spectroscopy measurements.^{11,46} The large singlet-triplet spin gap observed in the anion-order state can be related to the pattern of the charge ordering which accompanies the anion-ordering transition.⁴⁷ With higher charge density the coupling between neighboring spins increases. Hence, the charge-order pattern - o - O - o - along the stacks leads to a stronger dimerization ($d''_2 < d'_2$, see the insert in Fig. 8) and yields $J_1 \gg J_2$ with a very large value of Δ_σ ;⁴⁸ exactly as what is observed. It is interesting to note the similarity to ferroelectricity in one-dimensional organic quantum magnets, such as TTF-BA, where the polarization is changed by a magnetic field via a spin-Peierls transition.⁴⁹

V. CONCLUSIONS

We have performed a detailed magnetic characterization of the organic spin-chain compounds $(\text{TMTTF})_2\text{SbF}_6$, $(\text{TMTTF})_2\text{AsF}_6$, $(\text{TMTTF})_2\text{BF}_4$, $(\text{TMTTF})_2\text{ReO}_4$, and $(\text{TMTTF})_2\text{SCN}$ in the temperature range of 1.8 K up to 380 K using SQUID magnetometer and ESR experiments on single crystals. For $T \geq 100$ K the spin susceptibility at constant volume $(\chi_s)_V$ can be described as an $S = 1/2$ antiferromagnetic Heisenberg chain with exchange constants J between 400 K ($X = \text{SbF}_6$) and 460 K ($X = \text{SCN}$). In this family of compounds, J increases linearly with decreasing unit-cell dimension a along the chain. Charge localization and charge order, present in basically all of these salts, has no influence on the spin susceptibility. Below the spin-Peierls transition in $(\text{TMTTF})_2\text{AsF}_6$ ($T_{\text{SP}} = 13$ K) and the anion-ordering transition in $(\text{TMTTF})_2\text{BF}_4$ ($T_{\text{AO}} = 41$ K) the spin susceptibility can be described by Bulaevskii's model for alternating spin chain with singlet-triplet energy gaps of $\Delta_\sigma = 34.8$ and 52.0 K. The anion ordering in $(\text{TMTTF})_2\text{ReO}_4$ leads to a very large singlet-triplet gap $\Delta_\sigma = 1100$ K because a - o - O - O - o - charge pattern develops along the stacks in the anion-order state.

ACKNOWLEDGMENTS

We thank C. Bourbonnais, E. Rose, and D. Schweitzer for useful discussions. This work was supported by the Deutsche Forschungsgemeinschaft (DFG) and conducted within the Graduate College "Modern Methods of Magnetic Resonance in Materials Science" of Universität Stuttgart.

¹D. Jérôme and H. J. Schulz, *Adv. Phys.* **31**, 299 (1982).

²M. Dressel, *Naturwissenschaften* **90**, 337 (2003).

³M. Dressel, *Naturwissenschaften* **94**, 527 (2007).

⁴D. Jérôme, *Science* **252**, 1509 (1991).

⁵Also included is $(\text{TMTSF})_2\text{ClO}_4$ in the non-ordered phase which exhibits no anion ordering upon rapid cooling and thus becomes superconducting at ambient pressure.

⁶J. P. Pouget and S. Ravy, *J. Phys.* **6**, 1501 (1996).

⁷D. Chasseau, J. Gaultier, J. L. Miane, C. Coulon, P. Delhaes, S. Flandrois, J. M. Fabre, and L. Giral, *J. Phys. (Paris) Colloq.* **C3-44**, 1223 (1983).

⁸L. Ducasse, M. Abderrabba, J. Hoarau, M. Pesquer, B. Gallois, and J. Gaultier, *J. Phys. C* **19**, 3805 (1986).

⁹L. Ducasse, M. Abderrabba, B. Gallois, and D. Chasseau, *Synth. Met.* **19**, 327 (1987).

¹⁰T. Granier, B. Gallois, A. Fritsch, L. Ducasse, and C. Coulon, in *Lower Dimensional Systems and Molecular Electronics*, edited by R. M. Metzger, P. Day, and G. C. Papavassiliou (Plenum Press, New York, 1990), Vol. 248 of *NATO ASI, Series B: Physics*, p. 163.

¹¹C. Coulon, P. Delhaes, S. Flandrois, R. Langnier, E. Bonjour, and J. M. Fabre, *J. Phys. (France)* **43**, 1059 (1982).

¹²B. Köhler, E. Rose, M. Dumm, G. Untereiner, and M. Dressel, *Phys. Rev. B* (in press, 2011); e-print [arXiv:1011.2856](https://arxiv.org/abs/1011.2856).

¹³R. Moret, J. P. Pouget, R. Comes, and K. Bechgaard, *J. Phys. (Paris) Colloq.* **C3-44**, 957 (1983).

¹⁴C. Coulon, A. Maaroufi, J. Amiell, E. Dupart, S. Flandrois, P. Delhaes, R. Moret, J. P. Pouget, and J. P. Morand, *Phys. Rev. B* **26**, 6322 (1982).

¹⁵F. Iwase, K. Sugiura, K. Furukawa, and T. Nakamura, *Phys. Rev. B* **81**, 245126 (2010).

¹⁶R. Laversanne, J. Amiell, C. Coulon, C. Garrigou-Lagrange, and P. Delhaes, *Mol. Cryst. Liq. Cryst.* **119**, 317 (1985).

¹⁷M. Dumm, A. Loidl, B. W. Fravel, K. P. Starkey, L. K. Montgomery, and M. Dressel, *Phys. Rev. B* **61**, 511 (2000).

¹⁸M. Dumm, A. Loidl, B. Alavi, K. P. Starkey, L. K. Montgomery, and M. Dressel, *Phys. Rev. B* **62**, 6512 (2000).

¹⁹L. K. Montgomery, in *Organic Conductors*, edited by J. P. Farges (Marcel Dekker, New York, 1994), p. 138.

²⁰F. Nad and P. Monceau, *J. Phys. Soc. Jpn.* **75**, 51005 (2006).

²¹B. Gallois, J. Gaultier, F. Bechtel, A. Filhol, L. Ducasse, and M. Abderrabba, *Synth. Met.* **19**, 321 (1987).

²²M. de Souza, P. Foury-Leylekian, A. Moradpour, J.-P. Pouget, and M. Lang, *Phys. Rev. Lett.* **101**, 216403 (2008).

²³M. Dressel, O. Klein, and S. Donovan, *Int. J. Infrared Millimeter Waves* **14**, 2489 (1993).

²⁴P. Wzietek, F. Creuzet, C. Bourbonnais, D. Jérôme, K. Bechgaard, and P. Batail, *J. Phys.* **3**, 171 (1993).

²⁵M. Dumm, M. Dressel, A. Loidl, B. W. Fravel, and L. K. Montgomery, *Physica B* **259-261**, 1005 (1999).

- ²⁶M. Dumm, M. Dressel, A. Loidl, B. W. Fravel, K. P. Starkey, and L. K. Montgomery, *Synth. Met.* **103**, 2068 (1999).
- ²⁷S. Eggert, I. Affleck, and M. Takahashi, *Phys. Rev. Lett.* **73**, 332 (1994).
- ²⁸J. C. Bonner and M. E. Fisher, *Phys. Rev.* **135**, A640 (1964).
- ²⁹W. E. Estes, D. Gavel, W. E. Hatfield, and D. Hodgson, *Inorg. Chem.* **17**, 1415 (1978).
- ³⁰M. Dressel, S. Kirchner, P. Hesse, G. Untereiner, M. Dumm, J. Hemberger, A. Loidl, and L. Montgomery, *Synth. Met.* **120**, 719 (2001).
- ³¹H. J. Schulz, *Int. J. Mod. Phys. B* **5**, 57 (1991).
- ³²J. Voit, *Rep. Prog. Phys.* **58**, 977 (1995).
- ³³F. Zwick, D. Jérôme, G. Margaritondo, M. Onellion, J. Voit, and M. Grioni, *Phys. Rev. Lett.* **81**, 2974 (1998).
- ³⁴R. Claessen, M. Sing, U. Schwingenschlögl, P. Blaha, M. Dressel, and C. S. Jacobsen, *Phys. Rev. Lett.* **88**, 096402 (2002).
- ³⁵The theoretical models are valid only above the phase transition, because the high transition temperature of $(\text{TMTTF})_2\text{ReO}_4$ ($T_{\text{AO}} = 156$ K) leads to a sharp decrease in the spin susceptibility.
- ³⁶C. Hotta, *Phys. Rev. B* **81**, 245104 (2010).
- ³⁷Y. Fuseya, M. Tsuchizu, Y. Suzumura, and C. Bourbonnais, *J. Phys. Soc. Jpn.* **76**, 014709 (2007).
- ³⁸Y. Tanaka and M. Ogata, *J. Phys. Soc. Jpn.* **74**, 3283 (2006).
- ³⁹S. Yasin, B. Salameh, M. Dumm, L. Montgomery, and M. Dressel (unpublished).
- ⁴⁰K. Furukawa, T. Hara, and T. Nakamura, *J. Phys. Soc. Jpn.* **78**, 104713 (2009).
- ⁴¹L. N. Bulaevskii, *Adv. Phys.* **37**, 43 (1988).
- ⁴²E. Orignac and R. Chitra, *Phys. Rev. B* **70**, 214436 (2004).
- ⁴³E. Pytte, *Phys. Rev. B* **10**, 4637 (1974).
- ⁴⁴M. Dumm, B. Salameh, M. Abaker, L. K. Montgomery, and M. Dressel, *J. Phys. IV* **114**, 57 (2004).
- ⁴⁵S. S. P. Parkin, J. J. Mayerle, and E. M. Engler, *J. Phys. Colloq.* **C3-44**, 1105 (1983).
- ⁴⁶G. Subias, T. Abbaz, J. M. Fabre, and J. Fraxedas, *Phys. Rev. B* **76**, 085103 (2007).
- ⁴⁷T. Nakamura, K. Furukawa, and T. Hara, *J. Phys. Soc. Jpn.* **75**, 013707 (2006).
- ⁴⁸Bulaevskii's model for an alternating spin chain (Ref. 40) shows that the singlet-triplet gap Δ_σ can be obtained by $\Delta_\sigma(0) = 0.43075(|J_1| + |J_2|)\delta^{2/3}$, where $(|J_1| + |J_2|)/2 = |J|$. Although this model is unable to fit our results, it agrees with our arguments concerning the relation between Δ_σ and the exchange constants J_1 and J_2 .
- ⁴⁹F. Kagawa, S. Horiuchi, M. Tokunaga, J. Fijioiko, and Y. Tokura, *Nature Phys.* **6**, 169 (2010).